REVIEW

Check for updates

Journal of
Sensor Science and Technology

The Korean Sensors Society

Encapsulation of Liquid Metal Particles for Next-Generation Stretchable Electronics

Sihun Lim[1], Jiho Kim[1], Donghyeon Kim[1], and Gun-Hee Lee[1,2,3,+]

[1]*Department of Optics and Mechatronics Engineering, Pusan National University, 2 Busandaehak-ro 63beon-gil, Geumjeong-gu, Busan, 46241, Republic of Korea*
[2]*Department of Cogno-Mechatronics Engineering, Pusan National University, 2 Busandaehak-ro 63beon-gil, Geumjeong-gu, Busan, 46241, Republic of Korea*
[3]*Crystael Bank Research Institute, Pusan National University, 2 Busandaehak-ro 63beon-gil, Geumjeong-gu, Busan, 46241, Republic of Korea*

Cite This: *J. Sens. Sci. Technol. Vol. 35, No. 1 (2026) 67-85*

https://doi.org/10.46670/JSST.2026.35.1.67

ABSTRACT: Stretchable electronic systems require conductive materials that maintain stable electrical performance under mechanical deformation. While bulk liquid metals offer metallic-level conductivity and exceptional deformability, their high fluidity and surface tension fundamentally limit the fidelity of patterning and operational stability. To address these challenges, liquid metal particles (LMP) have emerged as a promising alternative. In LMPs, the native oxide layer on the liquid metal particles stabilizes particle morphology and enables processability; however, this thin ceramic shell electrically insulates individual particles, preventing direct electrical contact. Moreover, the oxide layer alone provides insufficient mechanical integrity, necessitating the incorporation of an elastomeric or polymeric matrix to ensure mechanical stability under deformation. Consequently, both electrical activation and mechanical stabilization strategies are required to disrupt or bypass the oxide layer and establish percolating conductive networks. In particular, interfacial encapsulation of the oxide shell with various functional materials has recently emerged as an effective approach to simultaneously enhance electrical connectivity and mechanical robustness. This review summarizes recent advances in encapsulated LMP (eLMP)-embedded composites from a process–structure–property perspective, covering fabrication methods, interfacial and size-dependent mechanical effects, and electrical activation strategies. By linking processing conditions to microstructural design and macroscopic electrical and mechanical performance, this review provides a framework for the rational design of eLMP-based materials for next-generation stretchable electronic systems.

KEYWORDS: *Liquid metal particles, Interfacial encapsulation, Stretchable electronics, Soft electronics*

1. INTRODUCTION

Stretchable electronic systems, including wearable devices [1,2] and electronic skin [3,4], require conductive materials that can maintain stable electrical performance under mechanical deformation. Such systems must accommodate stretching, bending, and twisting while preserving sufficient electrical conductivity and mechanical reliability. Despite significant progress in materials and device engineering, achieving a combination of these properties remains a central challenge in the development of stretchable electronics.

Conventional metal conductors exhibit limited mechanical compatibility with soft substrates and often suffer from crack

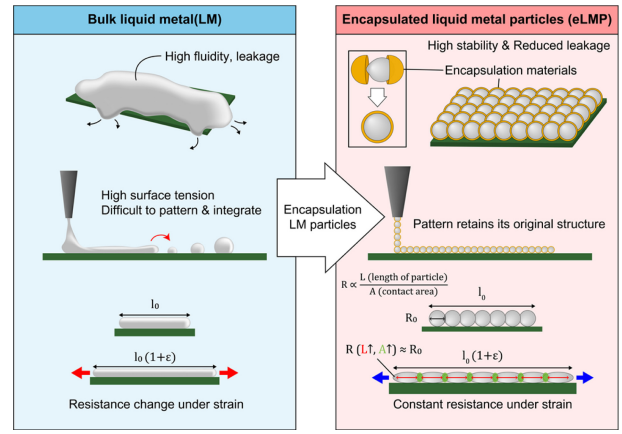

Fig. 1. Structural and electrical advantages of encapsulated liquid metal particle–based systems over bulk liquid metals.

+Corresponding author: gunheel@pusan.ac.kr
Received : Jan. 2, 2026, Revised : Jan. 8, Jan. 12, 2026, Accepted : Jan. 12, 2026

This is an Open Access article distributed under the terms of the Creative Commons Attribution Non-Commercial License (https://creativecommons.org/licenses/by-nc/3.0/) which permits unrestricted non-commercial use, distribution, and reproduction in any medium, provided the original work is properly cited.

formation, interfacial delamination, and fatigue-induced electrical degradation under repeated deformation [5]. Conductive polymers and elastomer-based composites offer improved deformability; however, their relatively low electrical conductivity restricts their use in applications that demand high electrical performance [6]. This trade-off between electrical conductivity and mechanical compliance has motivated the continued exploration of alternative conductive material systems.

Gallium-based liquid metals, such as eutectic gallium–indium (EGaIn) and Galinstan, have attracted attention as stretchable conductors owing to their combination of metallic-level conductivity with exceptional deformability and self-healing behavior [7]. However, the direct use of bulk liquid metals is hindered by their high fluidity and surface tension, which limit patterning fidelity, dimensional stability, and operational reliability [8]. These characteristics pose significant challenges to the integration of bulk liquid metals into scalable and mechanically stable electronic architectures.

To address these challenges, liquid metal particle (LMP)–based conductive fillers have been developed, in which bulk liquid metals are dispersed into micro- or nanoscale particles and encapsulated by a thin, ceramic native oxide layer. This particle-based architecture suppresses uncontrolled flow while significantly improving processability and compatibility with diverse printing and patterning techniques.

A defining characteristic of LMP-based systems is the spontaneous formation of a native oxide layer on the surface of the gallium-based liquid metal particles. This thin oxide shell stabilizes particle morphology and enables facile handling; however, it electrically insulates individual particles, thereby preventing spontaneous electrical percolation and restricting intrinsic conductivity [9].

Moreover, the native oxide shell alone provides insufficient mechanical integrity under repeated deformation. Accordingly, liquid metal particles are commonly embedded within elastomeric or polymeric matrices to achieve macroscopic structural stability. These material constraints suggest that LMP-based composites inherently present two interconnected design requirements: (i) electrical activation strategies to disrupt, penetrate, or circumvent the electrically insulating oxide layer, and (ii) mechanical stabilization strategies to preserve structural integrity under mechanical deformation.

More recently, interfacial encapsulation of liquid metal particles has emerged as an effective strategy to simultaneously address electrical activation and mechanical stabilization. In encapsulated liquid metal particle (eLMP)–based composites, functional materials—including polymers, elastomers, or conductive fillers—are deliberately engineered to conformally or selectively encapsulate the oxide shell of liquid metal particles. This interfacial encapsulation enhances electrical connectivity by promoting particle–particle contact or enabling conductive bridging, while concurrently improving mechanical robustness through strengthened particle–matrix interactions and reduced stress localization. Rather than treating the oxide layer solely as an obstacle to conductivity, eLMP-based approaches incorporate interfacial engineering as an integral component of composite design.

The performance of eLMP-based composites is strongly governed by processing conditions, interfacial architecture, and particle size–dependent effects. Fabrication strategies—including extrusion-based printing, photopolymerization-assisted lithography, evaporation-driven assembly, and hybrid manufacturing techniques—play critical roles in controlling particle organization, encapsulation uniformity, and composite microstructure. These structural factors collectively dictate electrical transport behavior, mechanical durability, and functional reliability under repeated mechanical deformation.

In this review, we focus on recent advances in eLMP-based composites and summarize progress from a process–structure–property perspective. We discuss representative fabrication strategies, interfacial and size-dependent mechanical effects, and electrical activation mechanisms specific to eLMP systems, thereby elucidating key design principles for stretchable electronic materials. By organizing recent developments within a unified conceptual framework, this review aims to facilitate the rational design of eLMP-based composites for next-generation stretchable electronic applications.

2. THE FABRICATION METHOD OF LIQUID METAL PARTICLES

Across a broad range of printing techniques, composite inks incorporating LMPs have emerged as a powerful platform for the fabrication of functional structures. By dispersing liquid metal into polymeric precursor matrices as the form of micro- or nanoscale droplets, these composite inks enable enhanced patterning controllability while simultaneously achieving structural stability and functional performance. Process precision has been substantially improved through strategies such as the surface chemical functionalization of liquid metal particles [16-18], the modulation of ink viscoelasticity [19,20], and the incorporation of photo- or thermally triggered curing mechanisms [16,21,22]. In this section, representative printing processes based on liquid-metal-containing composite inks are categorized according to their technological approaches, with an emphasis on ink formulations, curing and post-processing strategies, and the resulting structural characteristics and application potential.

ⓒ The Korean Sensors Society

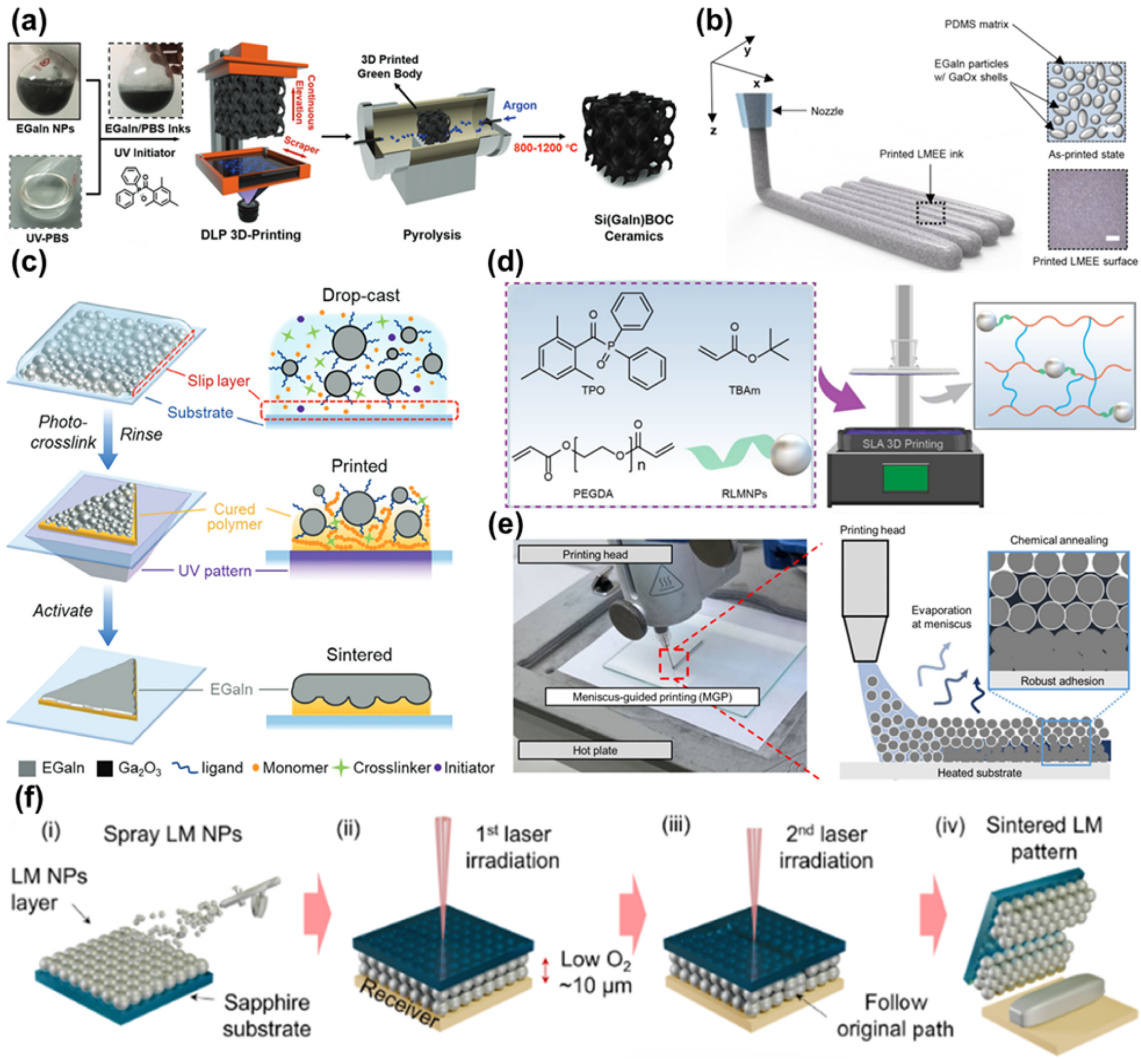

Fig. 2. Fabrication strategies for liquid metal particle–based composites. (a) DLP-Based 3D Printing and Pyrolysis of LM–Ceramic Composites. Adapted from Ref. [10]. (b) Direct Ink Writing of Liquid Metal–Embedded Elastomer (LMEE). Magnified dashed boxes indicate that the printable ink consists of EGaIn particles dispersed in a platinum-catalyzed PDMS matrix. Adapted from Ref. [11]. (c) Schematic of digital light processing (DLP)–based projection lithography. Adapted from Ref. [12]. (d) Fabrication process of 3D-printed structures using diphenyl(2,4,6-trimethylbenzoyl)phosphine oxide (TPO) as a photoinitiator, tert-butyl acrylate (TBAm) as the monomer, and poly(ethylene glycol) diacrylate (PEGDA) as the crosslinker. Adapted from Ref. [13]. (e) Schematic of meniscus guided printing (MGP) of polyelectrolyte-attached liquid metal microgranular-particle (PaLMP). Adapted from Ref. [14]. (f) The process of laser lift-off-and-fuse (LLOF). Adapted from Ref. [15].

Kong et al. reported the fabrication of complex three-dimensional ceramic metamaterials via a ceramic-conversion-based digital light processing (DLP) technique (Fig. 2(a)). A photocurable boron-containing siloxane (UV-PBS) resin, serving as a crosslinkable siloxane prepolymer, was employed as the matrix. Nanoscale liquid metal particles were generated by ultrasonication of EGaIn dispersed in tetrahydrofuran (THF) and were subsequently incorporated into the UV-PBS resin together with the photoinitiator Irgacure 1173. This formulation enabled selective photopolymerization using a DLP printer, allowing for the precise fabrication of three-dimensional architectures.

Following printing, the structures were pre-cured at 120°C and subsequently pyrolyzed at temperatures ranging from 800 to 1200°C under an argon atmosphere. During pyrolysis, organic components were removed, yielding a composite architecture composed of a Si(GaIn)BOC ceramic matrix interpenetrated by a GaIn metallic conductive network. The presence of the liquid metal significantly increased dielectric loss, resulting in excellent electromagnetic interference (EMI) shielding performance. Moreover, the viscoelastic nature of the liquid metal during thermal treatment mitigated structural shrinkage and contributed to the enhanced mechanical stability of the ceramic architectures.

ⓒ The Korean Sensors Society

Direct ink writing (DIW) represents another versatile printing approach, in which highly viscoelastic liquid-metal-based composite inks are extruded through a nozzle to construct three-dimensional structures at room temperature without the need for complex curing conditions. Ink viscosity is a critical parameter in DIW processes: excessively high viscosity leads to nozzle clogging, whereas insufficient viscosity compromises the shape fidelity and structural integrity of the printed features [23].Using this approach, Majidi et al. formulated a viscoelastic composite ink by shear mixing EGaIn particles into a platinum-catalyzed polydimethylsiloxane (PDMS) matrix and printed conductive structures via DIW (Fig. 2(b)). The printed structures initially exhibited insulating behavior due to the oxide shells surrounding the liquid metal particles. Upon the application of mechanical stimuli such as compression or stretching, selective rupture of the oxide layers occurred, establishing metallic interconnections between particles and activating electrical conductivity. This mechanically induced sintering mechanism enables the spatially and temporally programmable formation of conductive pathways, offering significant potential for reconfigurable circuits and flexible sensing applications [24].

Photopolymerization-based fabrication strategies further provide high resolution and rapid patterning capabilities for liquid metal composites, making them attractive for flexible electronics. He et al. demonstrated a hydrogen-bonding-assisted dispersion strategy using 2-hydroxyethyl acrylate (2-HEA) monomers, which interact with the Ga_2O_3 oxide layer on liquid metal particle surfaces (Fig. 2(c)). Upon the incorporation of a photoinitiator (Irgacure 819) and selective ultraviolet exposure, polymer structures with designed geometries were formed. Subsequent shear-induced activation enabledthe physical sintering of the liquid metal particles, while additional hydrogen bonding between the oxide layer and the polymer matrix during deformation ensured stable electrical performance.

In a related photopolymerization approach, Qiao et al. employed reversible addition–fragmentation chain transfer (RAFT) polymerization to synthesize liquid metal nanoparticles covalently grafted with polyacrylate chains, termed RAFT-modified liquid metal nanoparticles (RLMNPs). These surface-modified nanoparticles exhibited excellent dispersion stability within polymer resins. RLMNPs were uniformly dispersed in a photocurable resin containing tert-butyl acrylate (TBAm) monomers and poly(ethylene glycol) diacrylate (PEGDA) as a crosslinker, and composite structures were fabricated via stereolithography (SLA) using diphenyl(2,4,6-trimethylbenzoyl)phosphine oxide (TPO) as the photoinitiator (Fig. 2(d)).

Park et al. introduced meniscus-guided printing (MGP) using semi-solid-state polyelectrolyte-attached liquid metal microgranular particles (PaLMP). The PaLMP ink was prepared by tip-sonicating of liquid metal with polystyrene sulfonate (PSS) in an aqueous solution containing 10 vol% acetic acid (AA) (Fig. 2(e)). Unlike conventional droplet-based printing techniques, meniscus-guided printing (MGP) enables continuous film deposition through the controlled evaporation of the solvent at the moving meniscus formed between the nozzle and the substrate. In this evaporative regime, liquid metal microgranular particles are progressively assembled and densified along the contact line, allowing for the formation of uniform conductive patterns with high spatial resolution [25,26].

The successful implementation of MGP critically relies on the colloidal stability and rheological behavior of the ink. In this regard, the polyelectrolyte-attached liquid metal microgranular particles (PaLMP) play a pivotal role by preventing particle coalescence and nozzle clogging during printing, while simultaneously enabling dense particle packing during solvent evaporation. Moreover, the presence of acetic acid facilitates partial chemical annealing under heated substrate conditions, resulting in the localized disruption of the oxide shell and spontaneous electrical percolation, without requiring additional post-printing activation steps. As a result, this approach overcomes key limitations of conventional liquid-metal-based printing strategies, such as poor pattern fidelity and the need for mechanical or chemical activation, thereby enabling the rapid fabrication of highly conductive and mechanically stable liquid metal patterns suitable for stretchable electronic applications.More recently, Deng et al. proposed a laser-driven transfer printing strategy for the fabrication of hyper-stretchable liquid metal electronics, which decouples pattern transfer from electrical activation through a two-step laser process (Fig. 2(f)). In this approach, nanoscale liquid metal particles were first prepared via ultrasonication and uniformly deposited onto a transparent sapphire donor substrate. The donor and an elastomeric receiver substrate were then assembled into a confined sandwich configuration with a microscale gap, enabling controlled laser-induced material transfer. Upon irradiation with a high-fluence near-infrared laser, localized vaporization of the liquid metal nanoparticles generated transient recoil pressure, resulting in the selective lift-off and transfer of patterned liquid metal units onto the receiver substrate without direct laser exposure of the polymeric surface.

Following the transfer step, a secondary laser scanning process with reduced fluence and increased spatial overlap was applied to the transferred patterns to induce in situ electrical activation. This low-energy laser treatment selectively disrupted the native oxide shells surrounding the liquid metal

ⓒ The Korean Sensors Society

nanoparticles, promoting interparticle coalescence and the formation of continuous metallic percolation pathways. By independently optimizing the laser fluence and scanning pitch for transfer and activation, this method enables precise control over pattern fidelity while minimizing thermal damage and oxidation-induced degradation. As a result, the printed liquid metal conductors exhibit high electrical conductivity, optical transparency, and exceptional stretchability exceeding 1000%, demonstrating the effectiveness of laser-driven transfer printing as a scalable, activation-free patterning strategy for next-generation soft and stretchable electronic systems.

Collectively, these printing strategies leverage the unique physicochemical properties of liquid metal particles to achieve multifunctional performance, including high fabrication precision, mechanically and electrically stable architectures, and adaptive responses to external stimuli.

3. INTERFACIAL AND SIZE-DEPENDENT EFFECTS IN LMP-POLYMER COMPOSITES

As discussed above, when incorporated into polymer matrices, LMPs exhibit electrical and thermal conductivities comparable to those of conventional metal–polymer composites, while providing superior stretchability and deformation stability. In addition, compared to bulk liquid metals, LMP-based systems offer enhanced stability, which has led to their widespread investigation. However, the use of LMPs as fillers requires the consideration of factors that differ from those relevant to bulk liquid metals or conductive solid fillers: (i) surface tension and (ii) the presence of a native oxide layer.

3.1 Surface tension

At micro and nanoscale dimensions, surface tension plays an increasingly significant role in liquid metals embedded within compliant polymer matrices. Classical Eshelby inclusion theory [29], which neglects interfacial surface energy and assumes homogeneous inclusions with idealized interfaces, generally predicts that liquid inclusions soften the host elastic matrix. However, as demonstrated by Dufresne et al. [27], this assumption breaks down when capillarity competes with elastic deformation at small length scales.

In this framework, the relative importance of surface tension is characterized by the elastocapillary length, defined as

$$L \equiv \frac{\Upsilon}{E} \tag{1}$$

where Υ denotes the interfacial surface tension, and E is the Young's modulus of the polymer matrix. When the particle radius R becomes comparable to or smaller than L

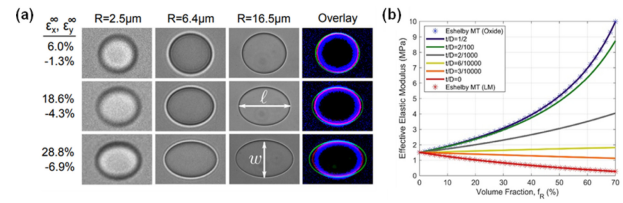

Fig. 3. Effect of LMP size in LMP-polymer composites (a) The deformation behavior of liquid inclusions with different radii under applied strain. Adapted from Ref. [27]. (b) The effect of the presence of an oxide layer on the effective elastic modulus of LMP–polymer composites based on a double-inclusion micromechanical model. Adapted from Ref. [28].

(i.e., $R \lesssim L$), surface tension significantly resists droplet deformation, leading to deviations from classical liquid inclusion behavior.

The deformation behavior of liquid inclusions with different radii under applied strain is shown in Fig. 3(a). While larger droplets exhibit pronounced elliptical deformation consistent with classical elastic predictions, smaller droplets remain nearly circular even at comparable strain levels. This suppression of deformation reflects the dominance of capillary forces at small length scales, where surface tension effectively constrains droplet shape.

In the capillarity-dominated regime, the effective stiffness of a liquid inclusion can be expressed through the interfacial-stiffness-modified modulus E_i,

$$E_i = E\frac{24\Upsilon}{10ER + 9\Upsilon'} \tag{2}$$

indicating that decreasing particle size or increasing surface tension leads to the apparent stiffening of the inclusion despite its liquid core. Incorporating this interfacial contribution into a micromechanical description yields the effective composite modulus E_C,

$$E_C = E\frac{1+\frac{2}{3}\frac{E_i}{E}}{\left(\frac{2}{3}-\frac{5}{3}\phi\right)\frac{E_i}{E}+\left(1+\frac{5}{3}\phi\right)'} \tag{3}$$

where ϕ is the volume fraction of liquid inclusions. This formulation captures the counterintuitive stiffening behavior observed in composites containing sufficiently small liquid inclusions—an effect that cannot be explained by classical Eshelby-type theories alone.

Consequently, in LMP–polymer composites, surface tension introduces a size-dependent transition between softening and stiffening regimes, governed by the interplay between particle radius, matrix modulus, and interfacial energy. These elastocapillary effects establish surface tension as a key design

ⓒ The Korean Sensors Society

parameter for tailoring mechanical compliance and deformation stability in LMP-based composite systems.

3.2 Presence of an oxide layer

Gallium-based LM, such as eutectic gallium–indium (EGaIn), spontaneously forms a thin native oxide layer, typically on the order of 2–5 nm, upon exposure to ambient conditions. While this oxide layer has a negligible influence on bulk liquid metals, it becomes a critical factor for LMPs, where the oxide constitutes a non-negligible interphase at the micro- and nanoscale.

As discussed earlier, classical Eshelby inclusion theories treat inclusions as homogeneous phases with idealized interfaces, leading to predictions that liquid inclusions primarily soften the surrounding elastic matrix. In LMP systems, however, the formation of an oxide shell introduces a core–shell inclusion geometry that deviates fundamentally from this assumption. The liquid core is mechanically constrained by the oxide layer, giving rise to size-dependent mechanical behavior that cannot be captured by classical liquid-inclusion models.

As demonstrated by Malakooti et al. [28], using a double-inclusion micromechanical model, the influence of the oxide layer becomes increasingly pronounced as particle size decreases and can be conveniently described by the ratio of oxide layer thickness t to particle diameter D.

This effect is illustrated in Fig. 3(b), which presents predictions of the effective elastic modulus of LMP–polymer composites based on a double-inclusion micromechanical model. In the absence of an oxide layer (t/D = 0), the composite behavior follows the classical prediction for liquid inclusions, exhibiting monotonic softening with increasing filler volume fraction. In contrast, even modest increases in t/D lead to a pronounced stiffening response, with the effective modulus approaching or exceeding that of the matrix at sufficiently high volume fractions. These results demonstrate that, despite its nanometric thickness, the oxide layer can dominate the macroscopic mechanical response when the inclusion size is sufficiently small.

This trend is especially evident in softer matrices, where the effective modulus increases rapidly with the oxide thickness ratio compared to stiffer matrices, highlighting the enhanced role of the oxide shell under compliant elastic conditions. A similar amplification effect is expected for surface-tension-driven stiffening, as interfacial capillary forces become increasingly dominant with decreasing matrix modulus.

Accordingly, the native oxide layer plays a central role in LMP-based composites, acting as a key parameter that governs size-dependent mechanical reinforcement, deformation stability, and deviations from classical inclusion theory.

3.3 Liquid metal particle-polymer composite

As discussed above, polymer composites incorporating LMP exhibit excellent electrical, mechanical, thermal, and optical properties, enabling their use in a wide range of applications such as stretchable electronics, wearable devices, and soft robotic systems [30-34].

LMP-embedded polymer composites have been widely explored as stretchable conductors in stretchable and deformable electronics because LM inclusions can accommodate large mechanical deformations while maintaining electrical conductivity [35,36]. Unlike rigid metallic fillers, liquid metal particles deform reversibly, often adopting ellipsoidal shapes under tensile strain, thereby preserving particle–particle contacts and minimizing the disruption of the conductive network. As a result, LMP-based conductors typically exhibit minimal resistance variation under large strain, making them particularly attractive for stretchable interconnects, soft circuit traces, and wearable electronic platforms [37,38].

Park et al. demonstrated stretchable conductors based on ligand-fuctionalized liquid metal particles that combine high electrical conductivity with strain-invariant performance under large deformation [44]. The conductive pathways remain stable and confined within the elastomer matrix, suppressing liquid metal leakage and ensuring reliable electrical performance under deformation. Kang et al. reported an elastic printed circuit board (E-PCB) enabled by an acoustically assembled liquid metal particle network (LMPNet). In their approach, an initially insulating LMP–polymer composite is first patterned and subsequently converted into a highly conductive network via a brief acoustic-field treatment, which generates nanoscale liquid metal particles (~100 nm) at the surface of pre-existing microscale LMPs that bridge neighboring particles to form a densely interconnected percolation network without observable leakage. Importantly, these nanoscale interconnectors do not merely provide electrical bridges; they also enhance toughness by introducing an additional energy-dissipation mechanism. Under tensile deformation, the microscale LMPs elongate into ellipsoidal shapes while the nanoscale interconnectors preserve particle–particle contacts, resulting in metallic-level conductivity (~10^6 S/m) with negligible resistance change under large strain and cyclic stretching. Leveraging these properties, the authors demonstrated a system-level E-PCB in which LMPNet traces serve as elastic interconnects for high-density micro-LED arrays and more complex electronic assemblies, maintaining

ⓒ The Korean Sensors Society

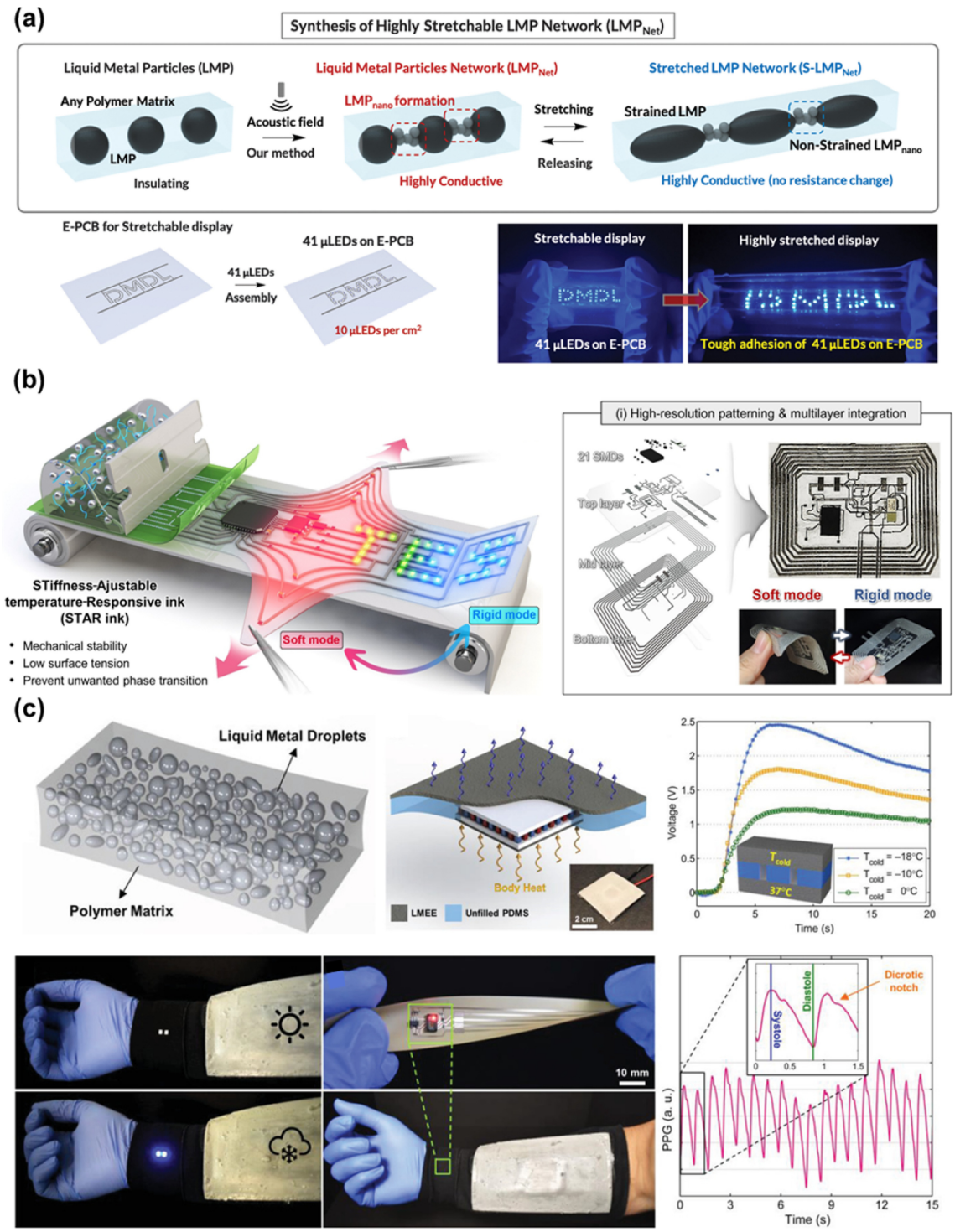

Fig. 4. Stretchable electronic applications of LMP-polymer composites (a) Acoustically assembled LMP network (LMPNet) enabling elastic printed circuit boards and micro-LED integration with highly strain-insensitive conductivity. Adapted from Ref. [39]. (b) pH-controlled chemically sintered phase-change metal "STAR ink" showing reversible soft–rigid switching while retaining high conductivity. Adapted from Ref. [40]. (c) Supercooled liquid metal droplets embedded in PDMS for sub-zero-tolerant soft interfaces and wearable thermoelectric demonstrations. Adapted from Ref. [41].

stable operation before and after stretching (Fig. 4(a)).

LMP-embedded polymer composites are particularly well suited for stiffness-switchable materials, as liquid metals can undergo reversible phase transitions between liquid-like and solid-like states near ambient conditions while maintaining electrical conductivity [45-49]. This unique combination

ⓒ The Korean Sensors Society

enables large, discontinuous changes in mechanical stiffness without sacrificing electrical functionality, making LMP-based systems particularly attractive for applications that require mechanical adaptability, such as soft–rigid hybrid electronics, reconfigurable circuits, and mechanically stable electronic packaging.

Liu et al. reported a lightweight liquid metal skeleton embedded in elastomer matrices, in which the liquid-to-solid phase transition of gallium-based particles induces a substantial increase in structural stiffness while preserving continuous electrical pathways [50]. Jeong et al. developed a STiffness-Adjustable Temperature-Responsive (STAR) ink based on pH-controlled chemical sintering, which enables the formation of conductive networks without inducing undesired phase transitions or liquid metal leakage [40]. As a result, the composite exhibits a reversible transition from a compliant state to a mechanically rigid state. The Young's modulus of the printed structures changes dramatically from approximately 552 kPa in the soft state to ~107 MPa in the rigid state, corresponding to an increase of nearly 200-fold, allowing the composite to transition between deformation-tolerant and mechanically robust configurations. Despite this large change in mechanical stiffness, the printed conductors retain metallic-level conductivities of approximately 2.27×10^6 S m^{-1} in the rigid state and 1.78×10^6 S m^{-1} in the soft state. As demonstrated in Fig. 4(b), this tunable mechanical response enables circuits to operate reliably across both soft and rigid modes, highlighting the potential of LMP–polymer composites as active mechanical elements in adaptive electronic systems.

LM droplet–elastomer composites combine the high thermal conductivity of LM with the conformal compliance of soft polymers, enabling efficient heat transfer in wearable and low-temperature environments [51-53]. Gong et al. showed that elastomers containing dispersed liquid-metal droplets retain enhanced thermal conductivity even under large tensile deformation, as the liquid droplets deform and reconfigure with the matrix rather than fracturing the thermal pathways [54]. As a result, efficient heat transport is maintained in both relaxed and stretched states, which is particularly advantageous for deformable and wearable thermal-management applications. Majidi et al. developed a liquid-metal-embedded elastomer (LMEE) in which liquid metal droplets dispersed within a PDMS matrix exhibit a pronounced supercooling effect, remaining liquid well below the freezing point of bulk EGaIn (Fig. 4(c)). As a result of this supercooling behavior, the crystallization peak is suppressed from approximately −5.9°C to −84°C, while the melting peak shifts from +17.8°C to −25.6°C, allowing the composite to retain mechanical softness and stretchability under sub-zero conditions. Based on these properties, they implemented the LMEE as a compliant thermal interface layer positioned between thermoelectric modules and skin-mimicking substrates, enabling intimate mechanical contact and efficient heat transfer across deformable surfaces. In this configuration, an unfilled PDMS layer was additionally introduced as a thermal barrier to reduce unintended heat transfer and energy dissipation. Leveraging this thermally efficient and mechanically stable interface, they subsequently demonstrated a self-powered thermoelectric sleeve that harvests body heat to drive light-emitting diodes and a pulse-oximeter circuit. Stable electrical output was maintained as the ambient temperature decreased from 0°C to −18°C, and the recorded photoplethysmogram (PPG) waveform exhibited clear systolic and diastolic peaks, confirming reliable bio-signal acquisition under mechanical deformation. Together, these results establish LMEE as a thermally resilient interface materials suitable for low-temperature and outdoor wearable electronic systems.

EGaIn-based nanoparticles possess superior photothermal transduction properties [55-58], enabling the efficient conversion of near-infrared light into localized heat. Recent studies have shown that such photothermal liquid metal nanoparticles can be directly integrated into photocurable resins to facilitate NIR-responsive 4D printing, where localized heating triggers shape-memory transitions and programmable deformation in printed structures [21]. As described in the processing section, Qiao et al. prepared RAFT-modified liquid metal nanoparticles (RLMNPs), in which diphosphonic-acid-terminated RAFT agents coordinatively wrap the LMP surface, enabling stable dispersion in a photocurable acrylate resin and the fabrication of composite structures via stereolithography [13]. Fig. 5(a) highlights the functional consequence of this design: upon 808 nm NIR irradiation, the liquid metal phase within the RLMNPs generates a strong photothermal response, rapidly heating the printed composite above the polymer's glass transition temperature and activating the shape-memory transition. As a result, the printed structures undergo rapid and near-complete shape recovery from a programmed temporary shape. Furthermore, Zhang et al. demonstrated that selective NIR irradiation enables spatially controlled actuation, allowing for complex deformation behaviors. This capability suggests the potential of LMP–polymer composites for photothermally driven 4D actuation in soft robotic systems and other stimulus-responsive applications.

When LM is dispersed as discrete particles within an elastomeric matrix, the composite can exhibit a unique combination of electrical isolation and reconfigurability that is not accessible in bulk or pre-percolated liquid metal systems. In this particle-dispersed state, the liquid metal droplets remain electrically isolated from one another, rendering the composite globally insulating while retaining the ability to form

ⓒ The Korean Sensors Society

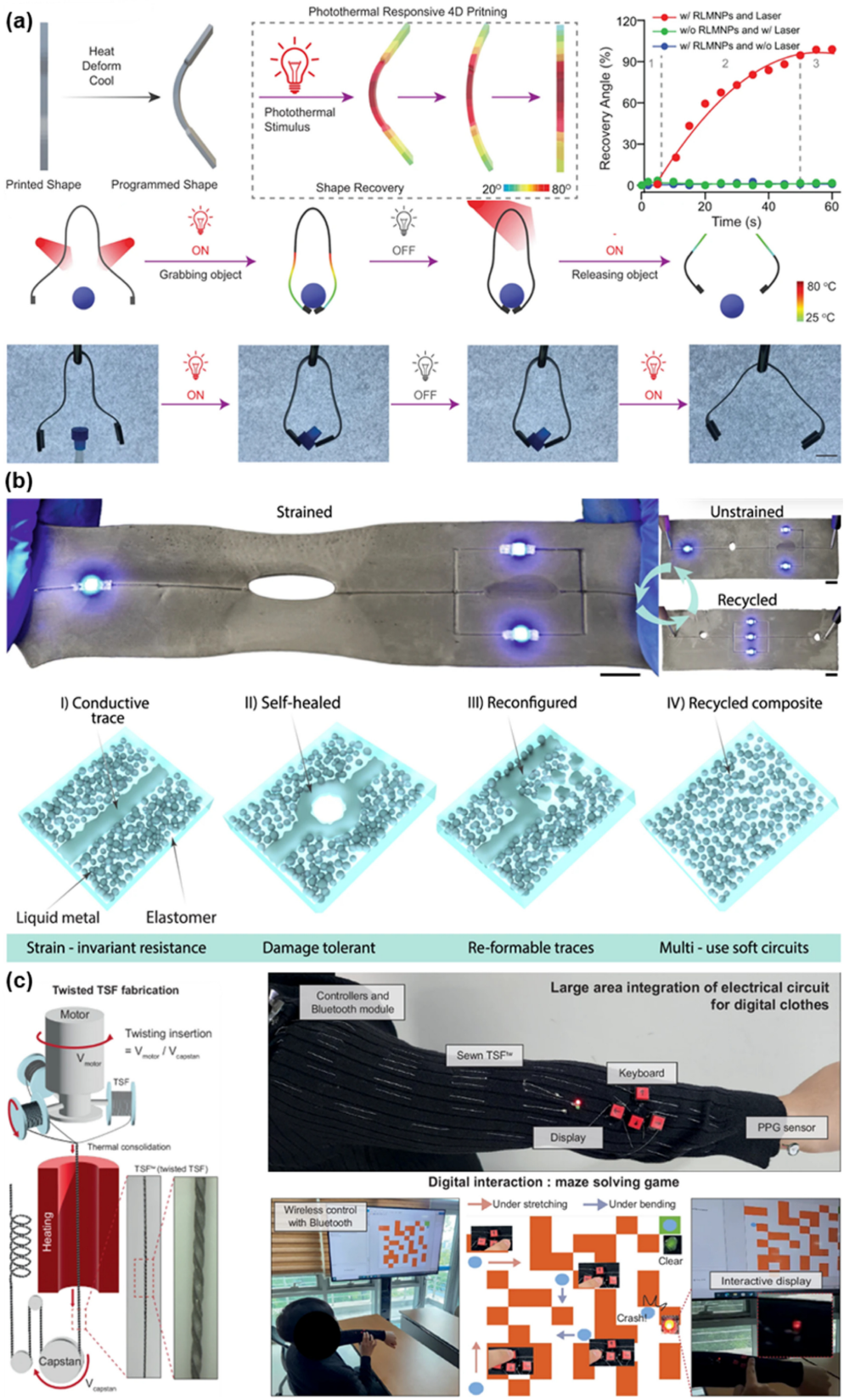

Fig. 5. Mechanically adaptive functionalities of LMP-polymer composites (a) NIR-triggered photothermal shape-memory actuation in SLA-printed RAFT-modified liquid metal nanoparticle composites. Adapted from Ref. [13]. (b) Damage-tolerant, self-healing, and rewritable LM–elastomer circuits formed by droplet rupture and coalescence. Adapted from Ref. [42]. (c) Meter-scale tough stretchable conductive fibers via heterostructure printing and twisting for textile-integrated electronics. Adapted from Ref. [43].

ⓒ The Korean Sensors Society

conductive pathways through external activation [24,59-63]. Yan et al. reported a pressure-programmable liquid-metal system based on a nanofibrous elastomer membrane containing semi-embedded liquid metal particles [64]. In the as-prepared state, the droplets are spatially confined within electrospun polymer fibers, maintaining an electrically insulating composite. Upon localized pressure stamping, only the exposed portions of the droplets rupture and flow into the fiber voids, selectively forming continuous conductive pathways while the surrounding regions remain insulating. Bartlett et al. demonstrated a self-healing and reconfigurable liquid metal–elastomer composite in which conductive pathways are selectively formed only in targeted regions via a localized mechanical embossing process (Fig. 5(b)). This mechanically induced activation forces neighboring liquid metal droplets to rupture interfacial barriers and coalesce into continuous conductive networks, while the surrounding particle-dispersed regions remain electrically insulating. Owing to the reconfigurable liquid metal microstructure, damaged traces autonomously restore electrical conductivity. Moreover, existing circuits can be locally erased and rewritten through solvent-assisted reconfiguration, in which localized toluene treatment disrupts the percolated liquid-metal network and electrically erases the conductive pathways, after which new traces can be re-formed by subsequent mechanical activation.

LMP-embedded polymer composites can be engineered to combine high electrical performance with exceptional toughness, enabling robust conductors that remain reliable under repeated deformation. Importantly, the polymer matrix not only provides mechanical reinforcement but also allows these composites to be processed into diverse form factors, including films, patterned traces, and filamentary architectures, without sacrificing electrical stability. Park et al. demonstrated meter-scale tough and stretchable conductive fiber (TSF) fabricated via the heterostructure printing of liquid metal particle–embedded thermoplastic polyurethane (TPU), followed by controlled twisting (Fig. 5(c)). During ink preparation, sonication-activated TPU conformally wraps the surface of liquid metal particles, forming a mechanically robust and leakage-free composite that markedly enhances toughness. Owing to their mechanical robustness and processing compatibility, these conductors were directly integrated into textile-based electronic systems, enabling large-area assemblies of functional components such as displays, keyboards, and biosensors that operate reliably during deformation and daily human motion. This capability was further demonstrated through a keyboard-based maze-solving game integrated into a digital garment, where stretchable conductors reliably transmitted user inputs and maintained stable electrical performance under stretching and bending during real-time interaction.

LMP composites can be engineered to exhibit diverse combinations of electrical, mechanical, and thermal properties. Such versatility enables their implementation across a wide range of functional systems, from deformable and wearable electronics to adaptive and stimulus-responsive devices. These studies collectively highlight the flexibility of LMP–polymer composites as a materials platform, while leaving ample room for further design and functional expansion in subsequent sections.

4. ELECTRICAL ACTIVATION OF LMP USING CONDUCTIVE MATERIALS

LMP-based systems offer advantages over bulk liquid metals in terms of microstructural control and process scalability [24]. However, they also suffer from a fundamental structural limitation: the native oxide layer formed on the particle surface restricts electrical connections between neighboring particles [65]. As individual LMPs remain electrically insulated, forming a continuous conductive pathway is difficult without an additional activation process. This limitation represents a primary obstacle to using LMPs as stretchable electrodes or interconnects [9,30].

An important implication of using LMPs in composite systems is that their functionality is not determined solely by the liquid metal core, but rather by how each particle is surrounded and interfaced with other materials. In practical LMP-based formulations, particles are rarely isolated; instead, they are embedded within, coated by, or connected through surrounding materials that govern electrical contact, mechanical constraint, and interfacial stability [66,67]. Therefore, developing functional LMP systems requires engineering not only the particles themselves but also the materials that envelop and mediate interactions between them [68].

Within this framework, conductive additives play a central role as functional materials that surround LMPs and define the interparticle interfaces [69]. Rather than directly removing the oxide layer, conductive additives can form electrically active shells, bridges, or networks around LMPs, enabling charge transport between neighboring particles [70]. By mediating interparticle contact through such surrounding conductive pathways, LMP systems can achieve intrinsic electrical conductivity without relying on aggressive mechanical sintering or thermal activation [65,71].

The advantages gained by introducing conductive additives arise from their ability to regulate LMP interfaces at multiple levels. Electrically, surrounding conductive materials provide continuous pathways between particles, helping to maintain stable resistance under deformation. Mechanically, they

ⓒ The Korean Sensors Society

constrain excessive liquid-metal flow and mitigate stress concentration, improving structural integrity during repeated stretching and bending [67]. From a processing perspective, conductive additives adjust ink viscosity and yield behavior, enabling the processing of LMP systems into printable formulations [9,71]. Additionally, surrounding conductive layers can enhance interactions between LMPs and polymer matrices or substrates, thereby contributing to improved adhesion and long-term reliability [14,72].

In this context, conductive additives should be regarded not as optional fillers but as essential design elements that functionalize LMPs by surrounding and interfacing them in a controlled manner. Depending on the dimensionality of the conductive additive (0D, 1D, or 2D) and the way it envelops or connects LMPs, distinct conduction mechanisms and deformation responses can be realized. Accordingly, additive-based strategies that engineer the surrounding conductive environment of LMPs have significantly expanded the application space of LMP-based composites [73]. This figure summarizes representative approaches based on conductive additives of different dimensionalities.

4.1 0D material additives

Zero-dimensional (0D) conductive materials have long been used as effective additives in composite systems owing to their ability to provide localized electrical contacts, fill interstitial gaps, and facilitate percolation at relatively low filler loadings [73,78,79]. Metallic particles and flakes offer high intrinsic conductivity and isotropic charge transport, making them well-suited for forming particle-level conductive junctions [70]. When introduced as conductive additives, 0D materials can therefore serve as efficient mediators of electrical connectivity while preserving the overall deformability of soft matrices [66,68].

Building on these advantages, recent efforts have explored the integration of 0D conductive materials with liquid metals or LMPs to overcome the electrical isolation imposed by the native oxide layer [24]. In such systems, 0D additives are employed to surround or occupy the gaps between LMPs, enabling particle-level electrical activation through percolation or metal–metal contact without requiring aggressive sintering processes [69-71]. The resulting 0D additive–LMP composites combine the fluidic deformability of liquid metals with the contact reliability of solid conductors, offering distinct advantages for soft electronics, stretchable interconnects, and printable electronic architectures. A representative example of this approach is a bi-phasic conductive elastomer ink prepared by blending Ag flakes and EGaIn into a styrenic block copolymer matrix, which extends liquid-metal-based materials to digital printing processes [74].

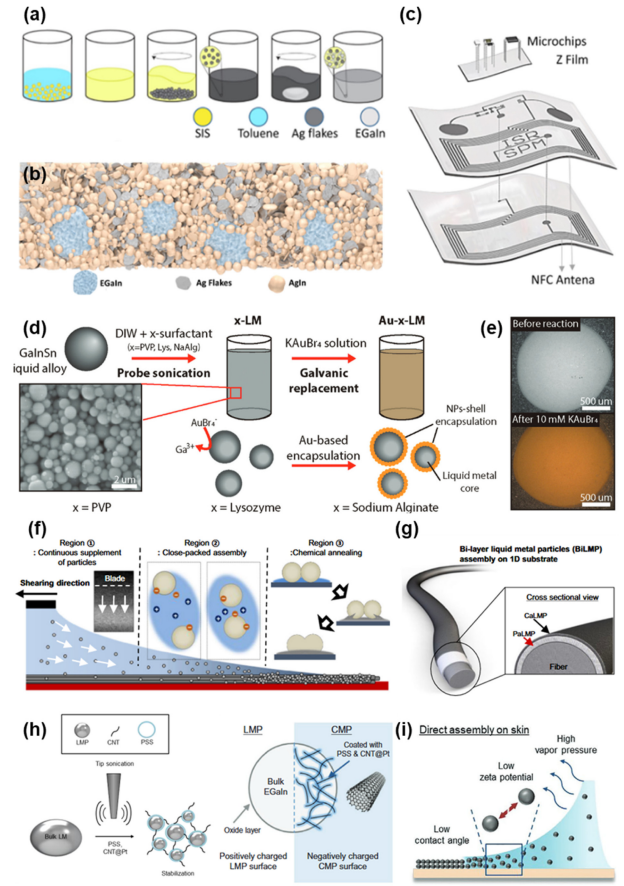

Fig. 6. Electrical activation of LMPs through the incorporation of 0D, 1D conductive materials. (a) Schematic illustration of a bi-phasic, printable elastomeric ink composed of Ag flakes and EGaIn dispersed in a styrenic block copolymer matrix. (b) Schematic model of the trinary microstructure. (c) Representation of a battery-free multi-layer NFC circuit, with a double-layer antenna for high-efficiency energy harvesting. Microchips are interfaced to the circuit using an anisotropic conductive film. Adapted from Ref. [74]. (d) Schematic representations of surface-engineered LMPs achieved via polymer-assisted surface modification followed by Au encapsulation through galvanic replacement. (e) Samples of LM droplets deposited on a carbon tape substrate before and after reaction. Adapted from Ref. [75]. (f) Illustration of a 1D bridging strategy in which carbon nanotubes (CNTs) facilitate interparticle electrical connection and mechanical stabilization during fiber coating. (g) Schematic illustration of BiLMP-coated fiber. The BiLMP-coated fiber consists of two layers: PaLMP (polymer-attached LMP) and CaLMP (carbon nanotube-attached LMP). Adapted from Ref. [76]. (h) Schematic of functionalized CNT(Pt-CNT) assisted composite metal particles, where electrostatic self-assembly and metal-metal interaction enable intrinsic conductivity without external activation. (i) Schematic illustration of direct coating of CMP on skin. Adapted from Ref. [77].

In this system, an SIS (styrene–isoprene–styrene) block copolymer is first dissolved in a solvent, Ag microflakes are dispersed, and EGaIn is added last to formulate an ink with

ⓒ The Korean Sensors Society

controlled viscosity. SIS serves as a highly elastic binder and tunes the rheological properties of the ink, allowing stable printing even with conventional extrusion-based printers (Fig. 6(a)).

Microstructural analyses indicate that the ink contains coexisting Ga–In droplets, Ag flakes, and newly formed $AgIn_2$ intermetallic compounds. SEM and EDS results show that microscale EGaIn droplets are surrounded by an oxide layer, with Ag flakes and $AgIn_2$ particles distributed around them. $AgIn_2$ can form even at room temperature because of the strong affinity between Ag and In, and these particles tend to concentrate at the droplet edges, acting as hinges that anchor the liquid metal [80,81]. This structure suppresses the excessive flow of the liquid metal while allowing the characteristic rearrangement of the liquid phase under tensile deformation, which helps maintain high stretchability (Fig. 6(b)).

A key aspect of the printing process is the rapid transition of the ink from a fluid-like to a mechanically stable state immediately after extrusion from the nozzle. This behavior originates from the physical crosslinking of the SIS block copolymer and the interactions between Ag flakes and EGaIn. Pure EGaIn tends to smear because of its low viscosity and high fluidity, whereas the combined introduction of Ag flakes and SIS gives the ink solid-like mechanical integrity, enabling direct writing without additional masking or encapsulation steps (Fig. 6(c)).

As a result, the Ag–In–Ga–SIS ink achieves an ultimate strain exceeding 600%, an electrical conductivity on the order of $\sim 7.0 \times 10^5\ S \cdot m^{-1}$, and a very low gauge factor (GF ≈ 0.9) even at 100% strain. The resistance change remains limited over repeated tensile cycling (>1000 cycles), indicating that this approach can combine the benefits of liquid metals with the mechanical stability of particle-filled composites [74].

However, this approach has limitations. First, a high Ag flake content can increase material cost. Second, reducing the SIS content to increase conductivity further may compromise printability and mechanical reliability. In addition, flake-based structures may undergo microstructural evolution during long-term use due to oxidation and intermetallic growth, which requires further validation under extended operating conditions. Still, this system serves as a useful reference case showing that liquid metal–particle–polymer hybridization can be extended to printable stretchable electronics.

Au encapsulation represents a surface-engineering strategy for activating LMPs, distinct from approaches that rely on dispersing external conductive fillers within a matrix. Rather than creating conductivity through filler-mediated percolation, this method directly transforms LMPs into electrically active units by forming metallic conduction pathways on their surfaces while preserving the native oxide layer [75].

In the reported approach, sub micrometer-scale LMPs are first generated via probe sonication in the presence of surfactants or stabilizing agents. These particles are subsequently exposed to an aqueous solution containing $AuBr_4^-$ ions, triggering a galvanic replacement reaction at the liquid metal interface. During this process, gallium at the particle surface is oxidized and dissolved as Ga^{3+}, while Au^{3+} ions are reduced in situ, leading to the nucleation and growth of Au nanoparticles on the LMP surface. As a result, a discontinuous yet electrically connectable Au nanoparticle shell forms around the liquid metal core [82,83].

A key characteristic of this system is the emergence of a biphasic core–shell structure, consisting of a deformable liquid metal core and a metallic nanoparticle shell. Although the Au shell does not form a fully continuous coating, electrical conduction is enabled when neighboring particles come into contact through Au–Au junctions. Importantly, during mechanical deformation, the liquid metal core can rearrange and redistribute stress, allowing the outer Au shells to maintain or recover electrical contact. This mechanism enables the formation of conductive networks without requiring mechanical sintering, external pressure, or post-processing activation steps (Fig. 6(d)).

Microscopic characterization further confirms the surface modification induced by galvanic replacement [84,85]. Before the reaction, the LMP surface appears smooth and featureless, while after exposure to $AuBr_4^-$, the surface becomes roughened and uniformly decorated with nanoscale features, consistent with the formation of an Au nanoparticle shell surrounding the liquid metal core (Fig. 6(e)).

From a functional perspective, Au-encapsulated LMPs can therefore be regarded as conductive building blocks rather than passive fillers. The electrical activity is intrinsically encoded at the particle level, which distinguishes this strategy from conventional composite-based approaches where conductivity emerges only after percolation or external activation. This particle-centric design also offers improved stability under repeated stretching and bending, as electrical continuity relies on reversible shell–shell contacts rather than permanent particle fusion [75].

Despite these advantages, several limitations remain. The use of Au introduces material cost concerns and may limit scalability for large-area applications. In addition, excessive or non-uniform growth of the Au shell can restrict the intrinsic deformability of LMPs and compromise their mechanical compliance. Precise control over reaction conditions is therefore essential to balance electrical connectivity with mechanical robustness. Nonetheless, Au encapsulation serves as a representative example demonstrating that surface chemistry alone can endow LMPs with electrical functionality, providing an important conceptual framework for particle-level activation strategies in liquid metal systems.

ⓒ The Korean Sensors Society

4.2 1D material additives

The 0D additive strategies discussed above focused on strengthening local particle-level contacts to activate LMP conductivity. In the Ag flake approach, many metal particles fill the gaps between LMPs to form percolation pathways, while in Au encapsulation, contact resistance is minimized by modifying LMPs with a metallic shell [74,75,86]. These approaches are effective for mitigating the oxide-layer issue and providing initial conductivity, but the conductive pathway formation still depends strongly on interparticle proximity and local contact conditions [68,87].

In deformable environments involving stretching, shear, or bending, interparticle distances change dynamically, and 0D contact alone often cannot maintain a continuous conductive network. This shifts the problem from a simple question of whether particles touch to the need for structural elements that can actively bridge particles. This motivation leads to strategies that use high-aspect-ratio 1D conductive materials as bridges.

Unlike 0D additives that rely on point contacts, 1D materials can form conductive pathways that span spatially separated particles. In other words, 1D additives provide intentionally designed bridging networks rather than leaving electrical connection to probabilistic contact, helping maintain conduction stability under deformation [88,89]. From this perspective, CNT- and Pt-CNT-based strategies can be viewed as a structural transition introduced to address the limitations of 0D additives [76,77].

In one representative study, carbon nanotubes (CNTs) were used as auxiliary conductive networks and mechanical reinforcements for LMPs. CNTs are 1D nanomaterials with a high aspect ratio and good electrical conductivity, enabling them to function as percolation bridges that physically connect LMPs [90,91]. Rather than using CNTs as the primary conductor, this system was designed in the form of CNT-attached LMPs (CaLMPs), so that CNT networks establish electrical pathways first upon particle contact. This configuration can bypass the initial insulation imposed by the oxide layer and provide initial conductivity without separate mechanical activation (Fig. 6(f)).

From a processing perspective, CaLMP inks were deposited onto fiber surfaces using suspension-shearing-based coating, enabling continuous particle supply through gravity and capillary flow and promoting evaporation-induced close packing [92,93]. In this process, CNTs act not only as additives but also as physical scaffolds that promote interparticle assembly, resulting in dense and continuous LMP packings along the fiber surface. Such structures offer a high packing density and adhesion stability that are difficult to achieve with conventional dip-coating or soaking methods (Fig. 6(g)).

Compared with a CNT network alone or a single LMP layer, the resulting architecture shows morphological features in which CNT-reinforced LMP assemblies are arranged as bilayer or composite-layer structures along the fiber surface. The CNT network suppresses network collapse under repeated stretching, bending, and friction, while mechanically supporting local LMP deformation and thereby reducing particle rupture and leakage. As a result, this approach can alleviate both the high gauge factor and conductivity degradation that often limit solid-filler-based fiber electrodes [76].

Park et al. introduced the Pt nanoparticle-decorated CNTs (CNT@Pt), rather than pristine CNTs, into LMPs to form composite metal particles (CMP; CNT-attached metal particles) with intrinsic conductivity without a separate mechanical activation step. During ultrasonication-based dispersion, LMPs become positively charged, while PSS-modified CNT@Pt becomes negatively charged, leading to electrostatically driven self-assembly. The CNTs do not simply wrap individual particles; instead, they form continuous networks spanning multiple LMPs, providing interparticle electrical bridges (Fig. 6(h)).

Importantly, introducing Pt goes beyond simple conductivity enhancement. Pt can act as a metal catalyst with a strong affinity for Ga at the LMP surface [88,94]. Analyses suggest that Pt is not confined to the CNT surface but can migrate to the LMP surface, promoting localized exposure and the diffusion of Ga beneath the oxide layer [95]. As a result, CMPs can form metallic conduction paths even when the oxide layer remains, which is a key distinction from simple CNT–LMP mixtures.

The CNT network also acts as a mechanical scaffold, helping maintain particle shape recovery and film integrity after compressive or shear deformation. CMP-based films were reported to show substantially improved resilience after compression as well as higher scratch and peel resistance compared with LMP-only films. These features are beneficial for applications such as skin-mounted electronics that undergo repeated deformation (Fig. 6(i)).

Overall, the Pt-CNT additive strategy is meaningful in that it addresses the LMP conductivity issue at the particle design stage rather than through post-activation. It shows that 1D-conductor-assisted LMP hybridization can be extended from a conductivity-improvement method to a structural design strategy that simultaneously supports electrical and mechanical stability [77].

4.3 2D material additives

While 1D conductive additives such as CNTs primarily

ⓒ The Korean Sensors Society

provide a linear bridge between (LMPs), the introduction of 2D conductive materials enables a fundamentally different mode of electrical activation based on contact-area expansion and interfacial control [98-100]. Owing to their planar geometry, 2D materials can interact with LMPs over extended interfaces, allowing electrical connectivity to be achieved not only through particle-to-particle bridging but also through collective structural reorganization. Recent studies have demonstrated that such 2D additives can be incorporated either at the particle level or directly into a continuous liquid-metal phase, leading to distinct mechanisms for controlling electrical and mechanical behavior [101].

A representative example of the latter approach is the integration of MXene into a continuous liquid-metal matrix to form so-called MXene/liquid metal plasticine (MLM). In this strategy, MXene is uniformly and stably dispersed within EGaIn via a solvent-assisted dispersion (SAD) process, without the need for chemical surface functionalization [102]. During SAD processing with a volatile solvent such as ethanol, the liquid metal undergoes repeated fragmentation and reintegration, while a transient slip layer forms around the MXene flakes. This process allows MXene to be gradually incorporated into the liquid metal without severe aggregation, ultimately yielding an interpenetrating bicontinuous structure composed of MXene and liquid metal (Fig. 7(a)).

The resulting MLM exhibits distinct rheological characteristics. As the MXene content increases, the viscosity rises sharply, and the liquid metal transitions from a freely flowing state to a non-flowing, plasticine-like material. For instance, introducing 0.25 wt% MXene increases the viscosity to approximately 8×10^4 Pa·s, while 3 wt% MXene leads to viscosities exceeding 8×10^5 Pa·s. At the same time, the system displays pronounced shear-thinning behavior, which preserves processability during blade coating and direct printing. This combination of high viscosity at rest and low viscosity under shear enables shape retention while maintaining printability [96].

Beyond rheological control, the MXene–liquid metal system demonstrates robust functional performance. Thin coatings prepared by the SAD method exhibit high electromagnetic interference (EMI) shielding effectiveness at relatively small thicknesses, with absorption loss dominating the shielding mechanism. The dual conductive network formed by MXene and liquid metal promotes multiple reflections and interfacial polarization, while maintaining mechanical stability under repeated stretching, elevated temperature exposure, and harsh environments. Collectively, these results indicate that MXene integration enables macroscopic control of liquid-metal behavior, effectively transforming liquid metal from a fluid conductor into a formable, printable, and bondable continuous material [96].

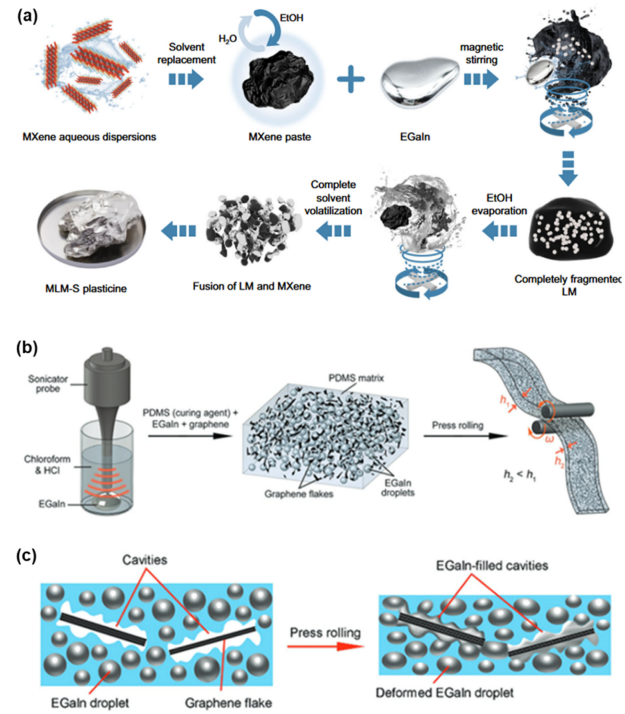

Fig. 7. Electrical activation of LMPs using 2D conductive materials. (a) MXene-integrated liquid metal system produced via solvent-assisted dispersion, forming a plasticine-like, printable, and highly conductive continuous phase through an interpenetrating MXene-LM network. Adapted from Ref. [96]. (b) Graphene flake-based 2D contact area expansion strategy where press-induced cavity collapse and droplet deformation activate conductive pathways between LMPs and graphene surfaces. (c) Schematic diagram demonstrating how the micro-nanocavities around the graphene flakes are filled with liquid metal after press-rolling. Adapted from Ref. [97].

In contrast to this continuous-phase strategy, graphene flake–based approaches operate primarily at the particle and composite level, where electrical activation is achieved through 2D contact-area expansion and cavity control. In these systems, EGaIn droplets and graphene flakes are co-dispersed within a polymer matrix, such as PDMS. Owing to the disordered stacking of graphene flakes, micrometer-scale void spaces (cavities) are formed, within which EGaIn droplets are initially confined. In this state, electrical connectivity remains limited by the native oxide layer on the liquid metal (Fig. 7(b)).

Upon mechanical press rolling, the cavities between graphene flakes progressively collapse, forcing the EGaIn droplets to deform in the planar direction and substantially increasing their contact area with the surrounding graphene surfaces [103,104]. During this process, the oxide layer locally rearranges, and multiple contact points are established between the liquid metal and graphene, leading to the activation of

ⓒ The Korean Sensors Society

conductive pathways [105]. Unlike 1D CNT-based strategies, graphene provides face-to-face interfacial contact, allowing the system to reach the percolation threshold under relatively low applied pressure (Fig. 7(c)).

As a result, a sharp increase in electrical conductivity is observed at relatively low graphene loadings, typically on the order of 0.6–1.0 wt%, which is significantly lower than those required in systems based solely on LMPs or graphene alone. After press rolling, the graphene–LMP composites exhibit electrical conductivities on the order of $10^3 - 10^4\ S \cdot m^{-1}$, and conductive pathways are maintained even beyond 100% tensile strain. Resistance changes remain relatively stable during repeated stretch–release cycles, indicating that graphene flakes not only provide electrical conduction but also mechanically assist the rearrangement and stabilization of LMPs.

Despite these advantages, graphene-based strategies also present limitations. Because graphene flakes are intrinsically stiff 2D solids, increasing their content tends to reduce the effective stretchability of the composite. Furthermore, electrical activation relies on an external mechanical process such as press rolling; extending this approach to freestanding structures or complex three-dimensional geometries remains challenging. In addition, since graphene–LMP interactions are predominantly physical rather than chemical, long-term cyclic deformation may induce interfacial rearrangements that affect electrical stability [97].

5. CONCLUSIONS

LMP–based composites have provided a practical route to overcome many of the limitations associated with bulk liquid metals in stretchable electronic systems. By dispersing liquid metals into discrete micro- or nanoscale particles and embedding them within polymeric matrices, these systems suppress uncontrolled flow and enable compatibility with diverse fabrication processes. At the same time, the presence of a native oxide layer on the liquid metal particles, while beneficial for morphological stability and processability, introduces inherent challenges related to electrical insulation and mechanical integrity under deformation.

Recent advances in eLMP-based composites highlight the importance of interfacial design in addressing these coupled challenges. By engineering functional materials to wrap or modify the oxide shell at the particle interface, eLMP-based approaches can simultaneously promote electrical connectivity and enhance mechanical robustness. Rather than relying solely on post-fabrication activation to disrupt the oxide layer, interfacial wrapping strategies integrate electrical activation and mechanical stabilization at the particle level, offering a more integrated and controllable design strategy for stretchable conductors.

Throughout this review, we have discussed how the performance of eLMP-based composites is governed by the interplay between fabrication processes, interfacial structure, and particle size effects. Processing routes such as extrusion-based printing, photopolymerization-assisted lithography, evaporation-driven deposition, and hybrid assembly methods play a critical role in governing particle organization, wrapping uniformity, and composite microstructure. These structural features, in turn, dictate macroscopic electrical behavior, mechanical durability, and functional reliability under mechanical deformation.

Despite significant progress, several challenges remain for the broader adoption of eLMP-based materials. Achieving precise and scalable control over particle size, wrapping uniformity, and interfacial chemistry in large-area manufacturing processes remains nontrivial. In addition, long-term reliability under cyclic deformation, environmental exposure, and complex loading conditions requires further systematic investigation. Addressing these issues will be essential for translating eLMP-based composites from laboratory demonstrations to practical device applications.

Looking forward, continued advances in interfacial engineering, materials chemistry, and process integration are expected to further expand the capabilities of eLMP-based systems. By establishing clear relationships between processing conditions, microstructural design, and macroscopic performance, eLMP-based composites offer a versatile platform for the rational design of stretchable electronic materials.

CRediT Authorship Contribution Statement

Sihun Lim: Investigation, Methodology, Writing - original draft. **Jiho Kim:** Writing - original draft. **Donghyeon Kim:** Writing - original draft. **Gun-Hee Lee:** Writing - review & editing, Supervision, Funding acquisition.

Declaration of Competing Interest

The authors declare that they have no known competing financial interests or personal relationships that could have appeared to influence the work reported in this paper.

Acknowledgements

This work was supported by he National Research Foundation of Korea [RS-2025-24682977] and a New Faculty Research Grant of Pusan National University, 2025.

ⓒ The Korean Sensors Society

REFERENCES

[1] J. Li, H. Jia, J. Zhou, X. Huang, L. Xu, S. Jia, et al., Thin, soft, wearable system for continuous wireless monitoring of artery blood pressure, Nat. Commun. 14 (2023) 5009.

[2] S. Kim, M. Saito, Y. Wei, P. Bhuyan, M. Choe, T. Fujie, et al., Stretchable and wearable polymeric heaters and strain sensors fabricated using liquid metals, Sens. Actuators A Phys. 355 (2023) 114317.

[3] L. Ding, C. Hang, S. Yang, J. Qi, R. Dong, Y. Zhang, et al., In situ deposition of skin-adhesive liquid metal particles with robust wear resistance for epidermal electronics, Nano Lett. 22 (2022) 4482–4490.

[4] Y. Peng, J. Song, Y. Zhang, H. Liu, J. Dong, H. Huang, et al., Permeable, wet-adhesive, and EMI-resistant liquid metal electronic skin for high-fidelity electrophysiological monitoring in sweaty and electromagnetic environments, Adv. Mater. 37 (2025) e08041.

[5] C. Cho, P. Kang, A. Taqieddin, Y. Jing, K. Yong, J.M. Kim, et al., Strain-resilient electrical functionality in thin-film metal electrodes using two-dimensional interlayers, Nat. Electron. 4 (2021) 126–133.

[6] S. Peng, Y. Yu, S. Wu, C.-H. Wang, Conductive polymer nanocomposites for stretchable electronics: material selection, design, and applications, ACS Appl. Mater. Interfaces 13 (2021) 43831–43854.

[7] Z. Zhao, S. Soni, T. Lee, C.A. Nijhuis, D. Xiang, Smart eutectic gallium–indium: from properties to applications, Adv. Mater. 35 (2023) 2203391.

[8] J. Ma, F. Krisnadi, M.H. Vong, M. Kong, O.M. Awartani, M.D. Dickey, Shaping a soft future: patterning liquid metals, Adv. Mater. 35 (2023) 2205196.

[9] M.D. Dickey, Stretchable and soft electronics using liquid metals, Adv. Mater. 29 (2017) 1606425.

[10] R. Xing, G. Xu, N. Qu, R. Zhou, J. Yang, J. Kong, 3D printing of liquid-metal-in-ceramic metamaterials for high-efficient microwave absorption, Adv. Funct. Mater. 34 (2024) 2307499.

[11] P. Won, C.S. Valentine, M. Zadan, C. Pan, M. Vinciguerra, D.K. Patel, et al., 3D printing of liquid metal embedded elastomers for soft thermal and electrical materials, ACS Appl. Mater. Interfaces 14 (2022) 55028–55038.

[12] D. Wu, S. Wu, P. Narongdej, S. Duan, C. Chen, Y. Yan, et al., Fast and facile liquid metal printing via projection lithography for highly stretchable electronic circuits, Adv. Mater. 36 (2023) 2307632.

[13] L. Zhang, X. Huang, T. Cole, H. Lu, J. Hang, W. Li, et al., 3D-printed liquid metal polymer composites as NIR-responsive 4D printing soft robot, Nat. Commun. 14 (2023) 7815.

[14] G.-H. Lee, Y.R. Lee, H. Kim, D.A. Kwon, H. Kim, C. Yang, et al., Rapid meniscus-guided printing of stable semi-solid-state liquid metal microgranular-particle for soft electronics, Nat. Commun. 13 (2022) 2643.

[15] Z. Ma, Y. Liu, J.-G. Hua, Y. Lei, T. Wang, L. Zhang, et al., Laser-driven transfer printing of hyper-stretchable liquid metal electronics, Adv. Electron. Mater. 11 (2025) e00244.

[16] S. Yang, H. Zhang, X. Sun, J. Bai, J. Zhang, 3D-printed liquid metal-in-hydrogel solar evaporator: merging spectrum-manipulated micro-nano architecture and surface engineering for solar desalination, ACS Nano 18 (2024) 5847–5863.

[17] Z. Song, J. Ma, R. Fang, J. Liu, H. Wang, Acidic-induced liquid metal–montmorillonite self-sintering conductive ink with multilayer sandwiched structure for flexible printed electronics, ACS Appl. Electron. Mater. 6 (2024) 3884–3893.

[18] S.-Y. Tang, R. Qiao, S. Yan, D. Yuan, Q. Zhao, G. Yun, et al., Microfluidic mass production of stabilized and stealthy liquid metal nanoparticles, Small 14 (2018) 1800118.

[19] M. Singh, P. Bhuyan, S. Jeong, S. Park, Directly printable, non-smearable and stretchable conductive ink enabled by liquid metal microparticles interstitially engineered in highly entangled elastomeric matrix, Adv. Funct. Mater. 35 (2024) 2412178.

[20] Z. Lin, X. Qiu, Z. Cai, J. Li, Y. Zhao, X. Lin, et al., High internal phase emulsions gel ink for direct-ink-writing 3D printing of liquid metal, Nat. Commun. 15 (2024) 4806.

[21] X. Huang, L. Zhang, J. Hang, T. Quinn, N.K.A. Nasar, Y. Lin, et al., 4D printing hybrid soft robots enabled by shape-transformable liquid metal nanoparticles, Adv. Mater. 36 (2024) 2409789.

[22] N. Corrigan, X. Shi, C. Boyer, Diblock copolymer stabilized liquid metal nanoparticles: particle settling behavior and application to 3D printing, ACS Macro Lett. 12 (2023) 241–247.

[23] O. Hur, R. Tutika, N. Klemba, E.J. Markvicka, M.D. Bartlett, Designing liquid metal microstructures through directed material extrusion additive manufacturing, Addit. Manuf. 79 (2024) 103925.

[24] S. Lee, S.A. Jaseem, N. Atar, M. Wang, J.Y. Kim, M. Zare, et al., Connecting the dots: sintering of liquid metal particles for soft and stretchable conductors, Chem. Rev. 125 (2025) 3551–3585.

[25] R.D. Deegan, O. Bakajin, T.F. Dupont, G. Huber, S.R. Nagel, T.A. Witten, Capillary flow as the cause of ring stains from dried liquid drops, Nature 389 (1997) 827–829.

[26] A.S. Dimitrov, K. Nagayama, Continuous convective assembling of fine particles into two-dimensional arrays on solid surfaces, Langmuir 12 (1996) 1303–1311.

[27] R.W. Style, R. Boltyanskiy, B. Allen, K.E. Jensen, H.P. Foote, J.S. Wettlaufer, et al., Stiffening solids with liquid inclusions, Nat. Phys. 11 (2015) 82–87.

[28] C. Chiew, M.H. Malakooti, A double inclusion model for liquid metal polymer composites, Compos. Sci. Technol. 208 (2021) 108752.

[29] J.D. Eshelby, The determination of the elastic field of an ellipsoidal inclusion, and related problems, Proc. R. Soc. A 241 (1957) 376–396.

[30] S. Chen, H.-Z. Wang, R.-Q. Zhao, W. Rao, J. Liu, Liquid metal composites, Matter 2 (2020) 1446–1480.

[31] Y. Deng, F. Bu, Y. Wang, P.S. Chee, X. Liu, C. Guan, Stretchable liquid metal based biomedical devices, npj Flex. Electron. 8 (2024) 12.

[32] S. Han, L. Chen, Y. Sun, Y. Guo, L. Bao, M. Gao, et al., Gallium-based liquid metals as an engineered

ⓒ The Korean Sensors Society

multifunctional platform: from biomedical innovations to energy and material systems, Adv. Funct. Mater. (2025) e00810.
[33] F.-C. Liang, B.C.K. Tee, Functional liquid metal polymeric composites: fundamentals and applications in soft wearable electronics, Adv. Funct. Mater. 34 (2024) 2400284.
[34] P. Won, S. Jeong, C. Majidi, S.H. Ko, Recent advances in liquid-metal-based wearable electronics and materials, iScience 24 (2021) 102698.
[35] R. Fang, B. Yao, T. Chen, X. Xu, D. Xue, W. Hong, et al., 3D highly stretchable liquid metal/elastomer composites with strain-enhanced conductivity, Adv. Funct. Mater. 34 (2024) 2310225.
[36] V. Vallem, V. Aggarwal, M.D. Dickey, Stretchable liquid metal films with high surface area and strain invariant resistance, Adv. Mater. Technol. 8 (2023) 2201233.
[37] G.G. Guymon, M.H. Malakooti, Multifunctional liquid metal polymer composites, J. Polym. Sci. 60 (2022) 1300–1327.
[38] A. Hoang, M. Grasinger, E.A. Papon, A. Koh, Exploring the complex deformation behavior of liquid metal polymer composites through experimental and novel computational approaches, Compos. Part B Eng. 296 (2025) 112257.
[39] W. Lee, H. Kim, I. Kang, H. Park, J. Jung, H. Lee, et al., Universal assembly of liquid metal particles in polymers enables elastic printed circuit board, Science 378 (2022) 637–641.
[40] S. Lee, G.-H. Lee, I. Kang, W. Jeon, S. Kim, Y. Ahn, et al., Phase-change metal ink with pH-controlled chemical sintering for versatile and scalable fabrication of variable stiffness electronics, Sci. Adv. 11 (2025) eadv4921.
[41] M.H. Malakooti, N. Kazem, J. Yan, C. Pan, E.J. Markvicka, K. Matyjaszewski, et al., Liquid metal supercooling for low-temperature thermoelectric wearables, Adv. Funct. Mater. 29 (2019) 1906098.
[42] R. Tutika, A.B.M.T. Haque, M.D. Bartlett, Self-healing liquid metal composite for reconfigurable and recyclable soft electronics, Commun. Mater. 2 (2021) 64.
[43] G.-H. Lee, Y. Lee, H. Seo, K. Jo, J. Yeo, S. Kim, et al., Meter-scale heterostructure printing for high-toughness fiber electrodes in intelligent digital apparel, Nat. Commun. 16 (2025) 4320.
[44] H. Seo, G.-H. Lee, J. Park, D.-Y. Kim, Y. Son, S. Kim, et al., Self-packaged stretchable printed circuits with ligand-bound liquid metal particles in elastomer, Nat. Commun. 16 (2025) 4944.
[45] H. Wang, S. Chen, X. Zhu, B. Yuan, X. Sun, J. Zhang, et al., Phase transition science and engineering of gallium-based liquid metal, Matter 5 (2022) 2054–2085.
[46] S. Gao, Y. Yang, A.S. Falchevskaya, V.V. Vinogradov, B. Yuan, J. Liu, et al., Phase transition liquid metal enabled emerging biomedical technologies and applications, Adv. Sci. 11 (2024) 2306692.
[47] Y. Hao, J. Gao, Y. Lv, J. Liu, Low melting point alloys enabled stiffness tunable advanced materials, Adv. Funct. Mater. 32 (2022) 2201942.
[48] H. Liu, Y. Xin, H.K. Bisoyi, Y. Peng, J. Zhang, Q. Li, Stimuli-driven insulator–conductor transition in a flexible polymer composite enabled by biphasic liquid metal, Adv. Mater. 33 (2021) 2104634.
[49] Q.-K. Nguyen, J. Ma, P. Zhang, Liquid metal-filled phase change composites with tunable stiffness: computational modeling and experiment, Mech. Mater. 183 (2023) 104702.
[50] J. Lu, B. Ma, G. Chen, Y. Chen, Y. Gao, Y. Chen, et al., Phase transition and mechanochemistry enabled lightweight liquid metal skeleton for multifunctional conductive composites, Adv. Compos. Hybrid Mater. 8 (2025) 261.
[51] M.D. Bartlett, N. Kazem, M.J. Powell-Palm, X. Huang, W. Sun, M.H. Malen, et al., High thermal conductivity in soft elastomers with elongated liquid metal inclusions, Proc. Natl. Acad. Sci. U.S.A. 114 (2017) 2143–2148.
[52] S. Wang, X. Zhao, J. Luo, L. Zhuang, D. Zou, Liquid metal (LM) and its composites in thermal management, Compos. Part A Appl. Sci. Manuf. 163 (2022) 107216.
[53] R. Zhang, M.-Y. Liu, W. Liu, Z.-M. Li, Z.-Z. He, Liquid metal-based elastomer heat conduction enhancement enabled by stretching, Case Stud. Therm. Eng. 43 (2023) 102801.
[54] C. Zhao, Y. Wang, L. Gao, Y. Xu, Z. Fan, X. Liu, et al., High-performance liquid metal/polyborosiloxane elastomer toward thermally conductive applications, ACS Appl. Mater. Interfaces 14 (2022) 21564–21576.
[55] X. Huang, L. Zhang, N.K.A. Nasar, L. Liu, X. Gu, Y. Lin, et al., Vat photopolymerization of liquid metal nanoparticle-integrated hydrogels, Adv. Funct. Mater. (2025) e23767.
[56] E. Miyako, Convergence of liquid metal biotechnologies for our health, Acc. Mater. Res. 2 (2021) 858–862.
[57] Y. Qi, M. Miyahara, S. Iwata, E. Miyako, Light-activatable liquid metal immunostimulants for cancer nanotheranostics, Adv. Funct. Mater. 34 (2024) 2305886.
[58] P. Zhu, S. Gao, H. Lin, X. Lu, B. Yang, L. Zhang, et al., Inorganic nanoshell-stabilized liquid metal for targeted photonanomedicine in NIR-II biowindow, Nano Lett. 19 (2019) 2128–2137.
[59] A.B.M.T. Haque, D.H. Ho, D. Hwang, R. Tutika, C. Lee, M.D. Bartlett, Electrically conductive liquid metal composite adhesives for reversible bonding of soft electronics, Adv. Funct. Mater. 34 (2024) 2304101.
[60] M. Kim, C. Cho, W. Shin, J.J. Park, J. Kim, P. Won, et al., Nanowire-assisted freestanding liquid metal thin-film patterns for highly stretchable electrodes on 3D surfaces, npj Flex. Electron. 6 (2022) 99.
[61] S. Liu, S.Y. Kim, K.E. Henry, D.S. Shah, R. Kramer-Bottiglio, Printed and laser-activated liquid metal-elastomer conductors enabled by ethanol/PDMS/liquid metal double emulsions, ACS Appl. Mater. Interfaces 13 (2021) 28729–28736.
[62] L. Tang, L. Mou, W. Zhang, X. Jiang, Large-scale fabrication of highly elastic conductors on a broad range of surfaces, ACS Appl. Mater. Interfaces 11 (2019) 7138–7147.
[63] J. Yang, P. Nithyanandam, S. Kanetkar, K.Y. Kwon, J. Ma, S. Im, et al., Liquid metal coated textiles with autonomous electrical healing and antibacterial properties, Adv. Mater. Technol. 8 (2023) 2202183.

ⓒ The Korean Sensors Society

[64] S. Zheng, X. Wang, W. Li, Z. Liu, Q. Li, F. Yan, Pressure-stamped stretchable electronics using a nanofibre membrane containing semi-embedded liquid metal particles, Nat. Electron. 7 (2024) 576–585.
[65] S. Liu, S.N. Reed, M.J. Higgins, M.S. Titus, R. Kramer-Bottiglio, Oxide rupture-induced conductivity in liquid metal nanoparticles by laser and thermal sintering, Nanoscale 11 (2019) 17615.
[66] Y. Ding, M. Zeng, L. Fu, Surface chemistry of gallium-based liquid metals, Matter 3 (2020) 1477–1506.
[67] S.-Y. Tang, R. Qiao, Liquid metal particles and polymers: a soft–soft system with exciting properties, Acc. Mater. Res. 2 (2021) 966–978.
[68] H. Bark, P.S. Lee, Surface modification of liquid metal as an effective approach for deformable electronics and energy devices, Chem. Sci. 12 (2021) 2760–2777.
[69] I.D. Tevis, L.B. Newcomb, M. Thuo, Synthesis of liquid core–shell particles and solid patchy multicomponent particles by shearing liquids into complex particles (SLICE), Langmuir 30 (2014) 14308–14313.
[70] M.D. Dickey, Emerging applications of liquid metals featuring surface oxides, ACS Appl. Mater. Interfaces 6 (2014) 18369–18379.
[71] Y. Lin, C. Cooper, M. Wang, J.J. Adams, J. Genzer, M.D. Dickey, Handwritten, soft circuit boards and antennas using liquid metal nanoparticles, Small 11 (2015) 6397–6403.
[72] S. Eristoff, A.M. Nasab, X. Huang, R. Kramer-Bottiglio, Liquid metal + x: a review of multiphase composites containing liquid metal and other (x) fillers, Adv. Funct. Mater. 34 (2024) 2309529.
[73] U. Daalkhaijav, O.D. Yirmibesoglu, S. Walker, Y. Mengüç, Rheological modification of liquid metal for additive manufacturing of stretchable electronics, Adv. Mater. Technol. 3 (2018) 1700351.
[74] P.A. Lopes, D.F. Fernandes, A.F. Silva, D.G. Marques, A.T. de Almeida, C. Majidi, et al., Bi-phasic Ag–In–Ga-embedded elastomer inks for digitally printed, ultra-stretchable, multi-layer electronics, ACS Appl. Mater. Interfaces 13 (2021) 14552–14561.
[75] R. David, N. Miki, Synthesis of sub-micrometer biphasic Au–AuGa2/liquid metal frameworks, Nanoscale 11 (2019) 21419–21432.
[76] G.-H. Lee, D.H. Lee, W. Jeon, J. Yoon, K. Ahn, K.S. Nam, et al., Conductance stable and mechanically durable bi-layer EGaIn composite-coated stretchable fiber for 1D bioelectronics, Nat. Commun. 14 (2023) 4173.
[77] G.-H. Lee, H. Woo, C. Yoon, C. Yang, J.-Y. Bae, W. Kim, et al., A personalized electronic tattoo for healthcare realized by on-the-spot assembly of an intrinsically conductive and durable liquid-metal composite, Adv. Mater. 34 (2022) 2204159.
[78] C. Votzke, U. Daalkhaijav, Y. Mengüç, M.L. Johnston, 3D-printed liquid metal interconnects for stretchable electronics, IEEE Sens. J. 19 (2019) 3832–3840.
[79] J. Tang, X. Zhao, J. Li, R. Guo, Y. Zhou, J. Liu, Gallium-based liquid metal amalgams: transitional-state metallic mixtures (TransM2ixes) with enhanced and tunable electrical, thermal, and mechanical properties, ACS Appl. Mater. Interfaces 9 (2017) 35977–35987.
[80] V. Simić, Ž. Marinković, Room temperature interactions in Ag-metals thin film couples, Thin Solid Films 61 (1979) 149–160.
[81] A.N. Campbell, W.F. Reynolds, The system silver–indium–gallium, Can. J. Chem. 40 (1962) 37–45.
[82] F. Hoshyargar, J. Crawford, A.P. O'Mullane, Galvanic replacement of the liquid metal Galinstan, J. Am. Chem. Soc. 139 (2017) 1464–1471.
[83] X. Li, M. Li, L. Zong, X. Wu, J. You, P. Du, et al., Liquid metal droplets wrapped with polysaccharide microgel as biocompatible aqueous ink for flexible conductive devices, Adv. Funct. Mater. 28 (2018) 1804197.
[84] X. Lu, J. Chen, S.E. Skrabalak, Y. Xia, Galvanic replacement reaction: a simple and powerful route to hollow and porous metal nanostructures, Proc. Inst. Mech. Eng. Part N J. Nanoeng. Nanosyst. 221 (2007) 1–16.
[85] K.D. Gilroy, P. Farzinpour, A. Sundar, R.A. Hughes, S. Neretina, Sacrificial templates for galvanic replacement reactions: design criteria for the synthesis of pure Pt nanoshells with a smooth surface morphology, Chem. Mater. 26 (2014) 3340–3347.
[86] W. Zu, Y. Ohm, M.R. Carneiro, M. Vinciguerra, M. Tavakoli, C. Majidi, A comparative study of silver microflakes in digitally printable liquid metal embedded elastomer inks for stretchable electronics, Adv. Mater. Technol. 7 (2022) 2200534.
[87] H. Lu, S.-Y. Tang, J. Zhu, X. Huang, H. Forgham, X. Li, et al., Nanoengineering liquid metal core–shell nanostructures, Adv. Funct. Mater. 34 (2024) 2311300.
[88] Y.-G. Park, H. Min, H. Kim, A. Zhexembekova, C.Y. Lee, J.-U. Park, Three-dimensional, high-resolution printing of carbon nanotube/liquid metal composites with mechanical and electrical reinforcement, Nano Lett. 19 (2019) 4866–4872.
[89] J.B. Andrews, K. Mondal, T.V. Neumann, J.A. Cardenas, J. Wang, D.P. Parekh, et al., Patterned liquid metal contacts for printed carbon nanotube transistors, ACS Nano 12 (2018) 5482–5488.
[90] W. Bauhofer, J.Z. Kovacs, A review and analysis of electrical percolation in carbon nanotube polymer composites, Compos. Sci. Technol. 69 (2009) 1486–1498.
[91] M. Moniruzzaman, K.I. Winey, Polymer nanocomposites containing carbon nanotubes, Macromolecules 39 (2006) 5194–5205.
[92] Y. Lin, J. Genzer, M.D. Dickey, Attributes, fabrication, and applications of gallium-based liquid metal particles, Adv. Sci. 7 (2020) 2000192.
[93] X. Gu, L. Shaw, K. Gu, M.F. Toney, Z. Bao, The meniscus-guided deposition of semiconducting polymers, Nat. Commun. 9 (2018) 534.
[94] H. Li, P. Tan, Y. Rao, S. Bhattacharya, Z. Wang, S. Kim, et al., E-tattoos: toward functional but imperceptible interfacing with human skin, Chem. Rev. 124 (2024) 3220–3283.
[95] F.-M. Allioux, M.B. Ghasemian, W. Xie, A.P. O'Mullane, T. Daeneke, M.D. Dickey, et al., Applications of liquid metals in nanotechnology, Nanoscale Horiz. 7 (2022) 141–

 ⓒ The Korean Sensors Society

167.
[96] H. Jiang, B. Yuan, H. Guo, F. Pan, F. Meng, Y. Wu, et al., Malleable, printable, bondable, and highly conductive MXene/liquid metal plasticine with improved wettability, Nat. Commun. 15 (2024) 6138.
[97] M.G. Saborio, S. Cai, J. Tang, M.B. Ghasemian, M. Mayyas, J. Han, et al., Liquid metal droplet and graphene co-fillers for electrically conductive flexible composites, Small 16 (2020) 1903753.
[98] X. Sun, H. Sun, H. Li, H. Peng, Developing polymer composite materials: carbon nanotubes or graphene?, Adv. Mater. 25 (2013) 5153–5176.
[99] N. Qureshi, V. Dhand, S. Subhani, R.S. Kumar, N. Raghavan, S. Kim, et al., Exploring conductive filler-embedded polymer nanocomposite for electrical percolation via electromagnetic shielding-based additive manufacturing, Adv. Mater. Technol. 9 (2024) 2400250.
[100] J. Jang, S.H. Lee, J. Kim, S.Y. Kim, S.H. Kim, Nano-bridge effect on thermal conductivity of hybrid polymer composites incorporating 1D and 2D nanocarbon fillers, Compos. Part B Eng. 222 (2021) 109072.
[101] N. Xu, S. Chen, Y. Li, N. Jiang, T. Zheng, N. Goossens, et al., A hybrid 1D/2D coating strategy with MXene and CNT towards the interfacial reinforcement of carbon fiber/poly(ether ether ketone) composite, Compos. Part B Eng. 246 (2022) 110278.
[102] M.R. Khan, C. Trlica, J.-H. So, M. Valeri, M.D. Dickey, Influence of water on the interfacial behavior of gallium liquid metal alloys, ACS Appl. Mater. Interfaces 6 (2014) 22467–22473.
[103] X. Gao, Y. Huang, X. He, X. Fan, Y. Liu, H. Xu, et al., Mechanically enhanced electrical conductivity of polydimethylsiloxane-based composites by a hot embossing process, Polymers 11 (2019) 56.
[104] B. Deng, P.-C. Hsu, G. Chen, B.N. Chandrashekar, L. Liao, Z. Ayitimuda, et al., Roll-to-roll encapsulation of metal nanowires between graphene and plastic substrate for high-performance flexible transparent electrodes, Nano Lett. 15 (2015) 4206–4213.
[105] J.N. Lee, C. Park, G.M. Whitesides, Solvent compatibility of poly(dimethylsiloxane)-based microfluidic devices, Anal. Chem. 75 (2003) 6544–6554.

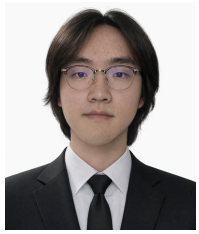

Sihun Lim is currently a B.S. degree in Optics and Mechatronics Engineering from Pusan National University. His research focuses on liquid-metal-based materials and devices for soft electronics and thermal management applications.

Gun-Hee Lee is currently an Assistant Professor in the Department of Cogno-Mechatronics Engineering at Pusan National University. He received his B.S. degree in Electrical and Electronic Engineering from Yonsei University and his Ph.D. degree in Materials Science and Engineering from KAIST. Before joining Pusan National University, he worked as a post-doctoral researcher in the Department of Mechanical Engineering at Carnegie Mellon University. His research focuses on soft materials engineering and bio-integrated machines.

ⓒ The Korean Sensors Society